Virology 483 (2015) 141–148

Contents lists available at ScienceDirect

Virology

journal homepage: www.elsevier.com/locate/yviro

RNA-binding residues in the N-terminus of APOBEC3G influence its DNA sequence specificity and retrovirus restriction efficiency

Kasandra Bélanger, Marc-André Langlois*

Department of Biochemistry, Microbiology and Immunology, Faculty of Medicine, University of Ottawa, Ottawa, Ontario, Canada

ARTICLE INFO

Article history:
Received 13 March 2015
Returned to author for revisions
1 April 2015
Accepted 15 April 2015
Available online 15 May 2015

Keywords:
APOBEC3G
Restriction factor
HIV-1
DNA deamination

ABSTRACT

APOBEC3G (A3G) is a host-expressed protein that inactivates retroviruses through the mutagenic deamination of cytosines (C) to uracils (U) in single-stranded DNA (ssDNA) replication products. A3G prefers to deaminate cytosines preceded by a cytosine (5′CC), whereas all other A3 proteins target cytosines in a 5′TC motifs. Structural and mutational studies have mapped the dinucleotide deamination preference of A3G to residues in loop 7 of the catalytic C-terminal domain of the protein. Here we report that A3G with a double W94A/W127A substitution in its N-terminus, designed to abolish RNA binding and protein oligomerization, alters the DNA deamination specificity of the enzyme from 5′CC to 5′TC on proviral DNA. We also show that the double substitution severely impairs its deaminase and antiretroviral activities on Vif-deficient HIV-1. Our results highlight that the N-terminal domain of the full length A3G protein has an important influence on its DNA sequence specificity and mutator activity.

Introduction

Retroviruses, such as HIV-1, can insert their genetic material into the genome of their host within only a few hours after entering a cell. To avoid damage or modifications to their genomic DNA, mammals have evolved several defense mechanisms against these unique pathogens. Members of the APOBEC3 (A3) family are deoxycytidine deaminases that present an important barrier to retroviral replication and spread in mammals (Reviewed in Desimmie et al., 2014; Harris and Dudley, 2015) There are seven A3 in humans, A3A to A3H, with each enzyme being characterized by the presence of one (A3A and A3C) or two (A3B, A3D, A3F and A3G) zinc (Z)-coordinating domains (Jarmuz et al., 2002; LaRue et al., 2009). There are three distinct types of Z domains in humans and primates, each containing a conserved $Hx_1Ex_{24-28}PCx_{2-4}C$ motif that constitutes a putative catalytic site in which the histidine and cysteines coordinate a zinc ion, whereas the glutamic acid acts as a proton shuttle. It is the hydrolytic attack of a zinc-activated water molecule on the C4 amine of the substrate deoxycytidine that results in the generation of a déoxyuridine (Neuberger et al., 2003). A3 proteins deaminate exclusively single-stranded DNA (ssDNA) (Harris et al., 2003; Suspene et al., 2004; Yu et al., 2004). The minus strand viral cDNA that is synthesized during the reverse transcription of retroviral genomic RNA is targeted and uracilated by A3 proteins. Uracils then template the insertion of adenosines (A) during the synthesis of the plus-strand proviral DNA thereby giving rise to G-to-A mutations. A high density of mutations, also called hypermutation, result in the incorporation of premature stop codons and protein defects that inactivate viral functions (Lecossier et al., 2003; Mariani et al., 2003).

The deaminase activity of A3 proteins is highly sequence-specific. A3G is the only enzyme of the family that strongly prefers to target cytosines (underlined) immediately preceded by a cytosine (5′CC), whereas all other A3 deaminate cytosines in a 5′TC motif (Beale et al., 2004; Dang et al., 2006; Doehle et al., 2005; Harris et al., 2003; Langlois et al., 2005; Liddament et al., 2004; OhAinle et al., 2006). Because the crystal structure of the full-length double-domain A3G protein has not yet been solved, there is an incomplete understanding of the global residues that influence target DNA specificity. Structurally, all A3 proteins share several conserved features including at least one Z domain consisting of five β-sheets surrounded by six α-helices (Bohn et al., 2013; Byeon et al., 2013; Chen et al., 2008; Kitamura et al., 2012; Siu et al., 2013). A recent study in which A3A and A3G residues were interchanged found that replacing D317 of the CTD of A3G, situated in loop 7 between β4 and α4, with the homologous tyrosine residue of A3A (Y132) was sufficient to alter the local dinucleotide preference for deamination from 5′CC to 5′TC (Rathore et al., 2013). Those results are supported by previous reports also implicating loop 7 residues in the dinucleotide deamination preference of several A3 proteins and also that of

* Correspondence to: Department of Biochemistry, Microbiology and Immunology Faculty of Medicine, University of Ottawa. 451 Smyth Road, Ottawa, Ontario, Canada, K1H 8M5. Tel.: +1 613 562 5800x7110.
E-mail address: langlois@uottawa.ca (M.-A. Langlois).

http://dx.doi.org/10.1016/j.virol.2015.04.019
0042-6822/

the activation-induced deaminase (AID) (Carpenter et al., 2010; Kohli et al., 2009, 2010; Langlois et al., 2005; Wang et al., 2010).

Because of its potent antiretroviral activity against a wide range of retroviruses, A3G is the best-characterized member of the A3 family. A3G has two Z domains (Z2-Z1) with each one containing a seemingly intact catalytic site, however only its C-terminal Z1 domain (CTD) is catalytically active (Hache et al., 2005; Navarro et al., 2005). The N-terminal domain (NTD) of the enzyme has been ascribed various other functions such as binding to HIV-1 Vif and virion encapsidation (Huthoff et al., 2009; Huthoff and Malim, 2007; Lavens et al., 2010; Mangeat et al., 2004; Schrofelbauer et al., 2004). Residues located in the NTD have also been implicated in nucleic acid binding, especially RNA (Bach et al., 2008; Bélanger et al., 2013; Bulliard et al., 2009; Huthoff et al., 2009; Iwatani et al., 2006; Khan et al., 2007; Shindo et al., 2012).

In addition to its cytosine deaminase activity, it is well established that A3G also has the ability, in certain experimental conditions, to hinder retroviral infection by means that are independent of deamination (Bélanger et al., 2013; Bishop et al., 2006, 2008; Guo et al., 2007; Iwatani et al., 2007; Li et al., 2007; Lu et al., 2015; Luo et al., 2007; Mariani et al., 2003; Mbisa et al., 2010; Newman et al., 2005; Wang et al., 2012). In particular, several groups have demonstrated defects in $tRNA_3^{Lys}$primer annealing and strand transfers during replication, which consequently lead to decreased levels of early and late reverse viral transcript accumulation as well as reduced proviral integration. Overall, these restriction mechanisms are thought to occur as a result of the direct interaction of A3G with the viral reverse transcriptase (RT) and integrase (IN), and possibly also through an alteration in the processivity of the reverse transcriptase caused by the clamping of A3G onto its ssDNA substrate during reverse transcription (Bishop et al., 2008; Luo et al., 2007; Wang et al., 2012). Recent work from our group has demonstrated that RNA binding by A3G is required for deamination-independent restriction (Bélanger et al., 2013). We mapped the RNA-binding ability of A3G to two tryptophans, W94 and W127, in the non-catalytic NTD of the protein. By individually substituting these two residues to alanine, A3G lost most deamination-independent functions including the inhibitions of late reverse transcript accumulation and proviral integration (Bélanger et al., 2013).

In this report we show that an RNA-binding defective mutant of A3G with two substitutions in its N-terminus, W94A/W127A, displays altered DNA substrate specificity. The loss of RNA-binding did not prevent the mutant enzyme from being incorporated into retrovirus virions, however its antiretroviral activity against a Vif-deficient HIV-1 pseudovirus was completely lost. Our observations support that the ability to bind RNA by full length A3G is required for retrovirus restriction and for high frequency provirus hypermutation. Surprisingly, the few hypermutated proviral sequences that were recovered from infected cells displayed a shift in the preferred target motif for deamination from 5′CC to 5′TC. This shift in target DNA specificity of the enzyme was also independently confirmed in a bacterial mutator assay where the double mutant was found to be as potent as the wild type A3G protein. This represents the first report to date showing the involvement of the NTD in the target specificity and regulation of A3G's mutator activity on a retrovirus.

Results and discussion

In a previous study we demonstrated that A3G [W94A] and A3G [W127A] mutants each had a significantly reduced ability to bind RNA, and more specifically, to 7SL, Alu, hY1 and hY3 RNAs (Bélanger et al., 2013). However, weak RNA binding could still be detected with these mutants. Here we were first interested to determine whether the double W94A/W127A substitution could account for all detectable RNA binding by A3G. Lysates from 293T cells transfected with Flag-tagged A3G or mutants were used for Co-IP using anti-Flag conjugated agarose beads followed by RNA isolation. Samples were then subjected to qPCR to measure the relative binding of each APOBEC to RNA. In these conditions, [W94A/W127A] did not bind to any of the RNAs tested above the background level set by the APOBEC2 (A2) negative control (Fig. 1A). A3G has a well-established ability to assemble into large oligomeric or high molecular mass (HMM) ribonucleic complexes (Chiu et al., 2005). In a previous report we showed that the W94A and W127A point mutants displayed a partial ability to assemble into oligomeric structure compared to wild type A3G (Bélanger et al., 2013). Here we analyzed the double mutant in presence and absence of RNase treatment. We could not detect any evidence of assembly into complexes that are RNA-dependent (Fig. 1B). Surprisingly, although RNA binding was lost, cytoplasmic foci believed to be P-bodies, stress granules and other RNA processing bodies that normally associate with A3G were still visible when similar levels of protein expression were compared (Fig. 1C and D) (Gallois-Montbrun et al., 2007; Kozak et al., 2006; Wichroski et al., 2006). This observation thereby indicates that association of A3G with these structures is not dependent on cellular RNA binding, nor is it dependent on protein aggregation or self-assembly (Fig. 1E).

We next investigated the impact of the double mutation on antiretroviral activity. Here we produced HIV [p8.9] pseudoviruses by co-transfecting viral expression plasmids along with A3G and various A3G mutants, including the catalytically inactive E259Q mutant and single point mutants W94A and W127A into 293T cells. We then confirmed by Western blot analysis that all the mutants, including [W94A/W127A], were expressed in 293T cells and were also efficiently packaged into virions, as judged by p24 capsid expression used for normalization (Fig. 2A). For reasons that are yet unclear, A3G mutants containing W94A or W127A point substitutions or the double substitution were all efficiently packaged into HIV [p8.9] pseudoviruses (Fig. 2A), but not into HIV-1 ΔV if viruses as would be expected (data not shown) (Bélanger et al., 2013). Consistent with our previous findings showing that the W94A and W127A point mutants displayed reduced antiretroviral activities (Bélanger et al., 2013), [W94A/W127A] was completely unable to restrict the infection of the virus (Fig. 2B).

Loss of the antiretroviral activity of the double mutants could be the result of protein misfolding causing defective deaminase activity. To evaluate the mutator activity of A3G [W94A/W127A] we conducted a bacterial mutator assay in *E. coli*. An increased frequency of rifampicin-resistant (Rif^R) colonies arises when A3G mutates the *rpoB* gene of *E.coli* rendering it resistant to rifampicin (Harris et al., 2002). Our results show that the full-length double mutant is well expressed in *E. coli* and generates similar frequencies of Rif^R colonies than wild type A3G (Fig. 2C and D) and (Table 1). Having confirmed that the double mutant's mutator activity is unaffected, we next investigated whether it could deaminate proviral DNA. Genomic DNA from 293T cells infected with viruses produced in presence of A3G and mutant proteins was isolated after 24 h. The eGFP reporter gene contained within the provirus was amplified by PCR and 120 clones were sequenced. None of the clones displayed G-to-A hypermutation in presence of the double mutant (data not shown). To determine whether there was a very low frequency of hypermutated sequences we next used 3D-PCR and HRM analysis (Bélanger et al., 2014; Suspene et al., 2005). These methods promote the selective PCR amplification (3D-PCR) or detection (HRM) of hypermutated sequences and provide qualitative information as to the intensity of the mutations. Results of these assays revealed the presence of mutations at intensities much lower than wild type A3G but similar to that of the single mutants (Fig. 2E and F) and (Table 1). No mutations were detected in the integrated proviral DNA of viruses produced in presence of A3G E259Q or A2. These results therefore indicate that the double mutant is capable of mutating provirus DNA, but at very low frequencies.

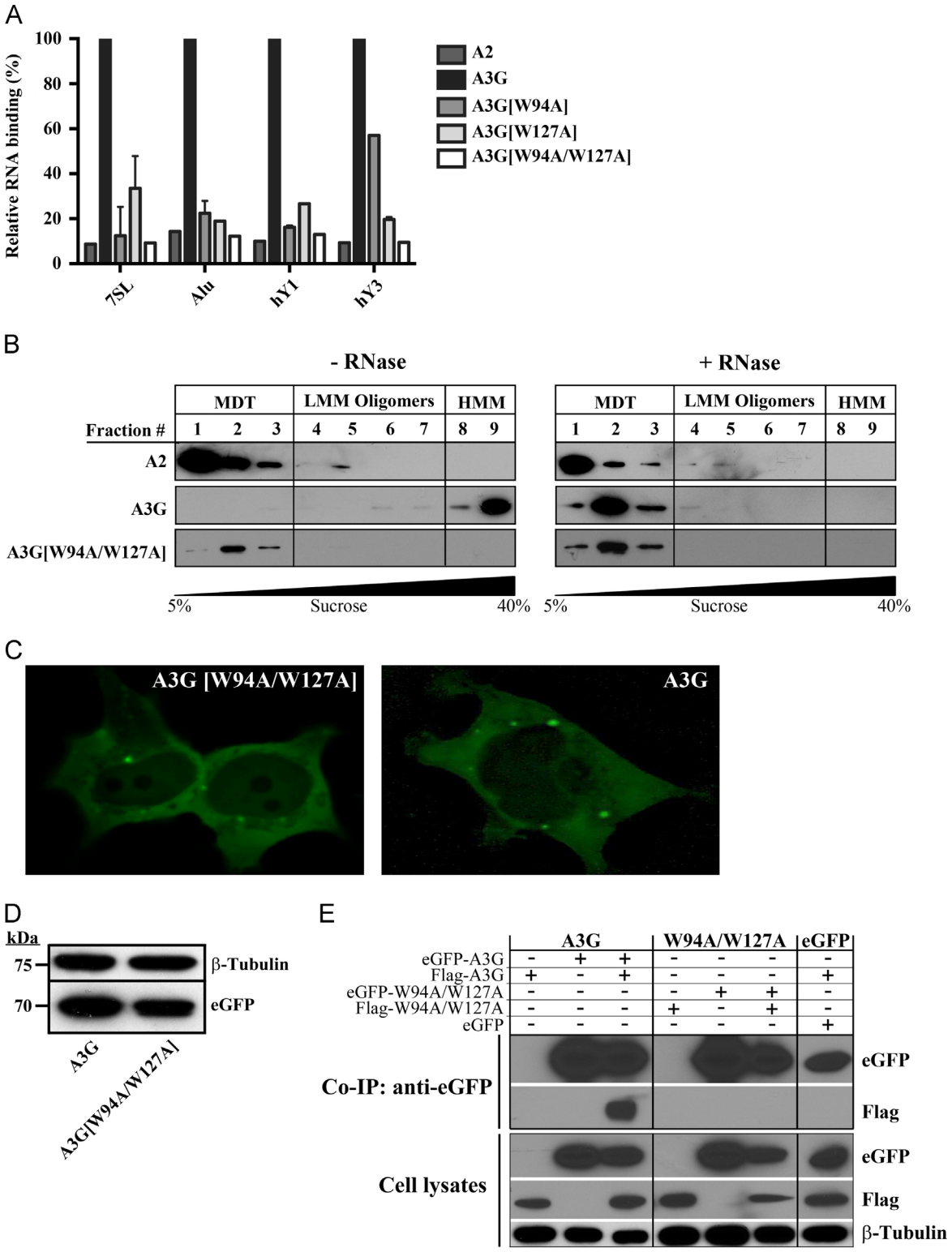

Fig. 1. Binding of A3G [W94A/W127A] to RNA and visualization of its subcellular localization. (**A**) Flag-A2, Flag-A3G or RNA-binding mutants of A3G were transfected in 293T cells. 48 h after transfection, cells were harvested, lysed in NP40 lysis buffer and subjected to Co-IP using anti-Flag-conjugated agarose beads. RNA was then isolated from immunoprecipitates and the binding of the different APOBECs to 7SL, Alu, hY1 and hY3 RNAs was determined by qPCR. Relative binding to A3G is depicted. Results represent the mean $\pm$ SD of triplicate values from three independent transfection experiments. (B) Lysates of transfected 293T cells, treated (right panels) or untreated with RNase A (left panels), were resolved by non-denaturing 5–40% sucrose gradient velocity ultra-centrifugation and analyzed by Western blot. Protein detection was performed with an anti-Flag antibody. MDT, monomers, dimers and tetramer; LMM, low molecular mass; HMM, high molecular mass. (C) eGFP-A3G and eGFP-A3G [W94A/W127A] expression plasmids were transfected in 293T cells and cultured in DMEM without phenol red for 48 h. Fluorescent images of the subcellular localization of the proteins were acquired with a 63X objective. (D) Cells transfected with eGFP-A3G or eGFP-A3G [W94A/W127A] were lysed 48 h after transfection and analyzed by Western blot using an anti-eGFP antibody; β-Tubulin was used as a loading control. (E) 293T cells were singly transfected (lanes 1, 2, 4 and 5) or co-transfected (lanes 3, 6 and7) with Flag- or eGFP-tagged APOBEC3 proteins. Pull-downs were carried out with anti-GFP magnetic beads. Homodimers were detected with an anti-Flag antibody (lanes 7–8).

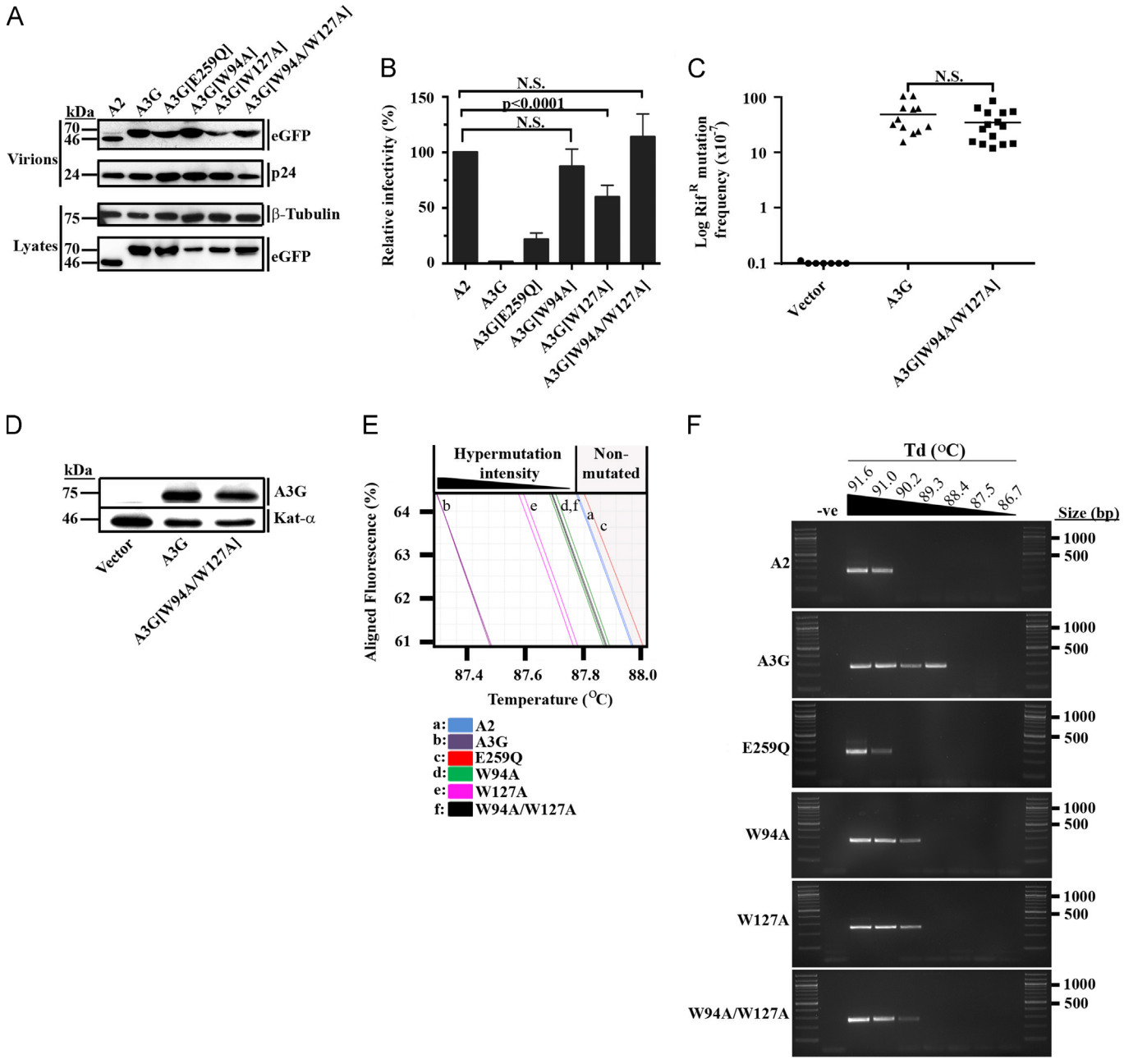

Fig. 2. A3G [W94A/W127A] hypermutates proviral DNA at a low frequency. (**A**) HIV [p8.9] viral particles produced in the presence of A3G or mutants of A3G were purified from cell supernatants, lysed and assayed for protein levels by Western blot analysis. Lysates of virus-producer cells are also presented. (B) Restriction of HIV [p8.9] infection by A3G and mutants as measured by flow cytometry in 293T target cells 24 h after infection. Results represent the mean ± SD of triplicate values from three independent transfection experiments. N.S., not significant. (C) Comparison of the mutator activities of A3G and A3G [W94A/W127A] in *E. coli.* Each point represents in Log the mutation frequency (Rif^R mutants per 10^7 viable cells) of an independent culture; the median values are indicated by a bar. Statistical significance was calculated using a two-tailed Student's *t*-test. (D) Western blot analysis performed on lysates of IPTG-induced bacterial cells used in the mutator assay described above. The expression of Kat-α was used as a loading control. (E and F) HIV [p8.9] viral particles produced in the presence of APOBEC proteins were used to infect 293T target cells. gDNA was extracted from infected cells 24 h after infection and used for (E) HRM analysis or (F) 3D-PCR analysis. (E) Duplicate melting curves for one representative experiment of three is shown. A2-treated samples (blue) delineate to the right a shaded region containing non-hypermutated sequences. PCR amplicons enriched in A/T content due to DNA deamination induce a shift in their melt curves towards lower temperatures. The linear segment of the melt-point threshold of the curve is presented for clarity. (F) 3D-PCR analyses. One representative experiment of three is shown. Amplification at lower temperatures is indicative of increased G-to-A hypermutation intensity.

We next analyzed the local DNA sequence context of the mutations in hypermutated proviral clones obtained by 3D-PCR. Our analysis revealed that the preferred dinucleotide DNA target site for A3G [W94A/W127A] had changed from 5′CC to a very firm 5′TC context (Table 2). We also observed a change in DNA deamination specificity at position -1 in a segment of the *rpoB* gene isolated from Rif^R *E. coli* colonies from a dominant 5′CC to 5′KC (where K is A or G) (Table 2 and Fig. 3) (Beale et al., 2004; Harris et al., 2003). Such a shift in deamination specificity to favor 5′TC is likely to further contribute to the low viral gene-inactivating potential of the mutant enzyme. An important part of the gene inactivation potency of A3G relies on the generation of TAG termination codons caused by deamination opposite to TGG tryptophan codons (Armitage et al., 2012). Weak mutational activity and frequency of mutated proviral DNA sequences combined to a 5′TC deaminase specificity would altogether highly compromise the antiretroviral activity of the A3G [W94A/W127A] protein.

Table 1
Mutation analysis in the eGFP gene of HIV [p8.9] and in the *rpoB* gene of *E. coli*.

APOBEC3	Sequences analyzed		Base pairs analysed[a]		G-to-A mutations		C-to-T mutations	
	eGFP	*rpoB*	eGFP	*rpoB*	eGFP	*rpoB*	eGFP	*rpoB*
A3G	5	33	1350	6534	29	2	0	28
A3G [W94A/W127A]	10	53	2700	10494	88	11	0	32

[a] The fragment analyzed in eGFP was 279 bp long whereas the *rpoB* fragment length was 198 bp.

Table 2
Local sequence preference for DNA deamination.

APOBEC3	HIV [p8.9]			*rpoB*		
	−2	−1	0	−2	−1	0
A3G						
A	24	–	–	–	3	–
C	38	76	100	87	67	100
T	24	24	–	3	23	–
G	14	–	–	10	7	–
A3G [W94A/W127A]						
A	24	2	–	3	16	–
C	26	6	100	67	12	100
T	26	92	–	16	42	–
G	24	–	–	14	30	–

Values represent the percentage of occurrence of each base at positions −1 and −2 respective to the deaminated cytidine (position 0). Sequence analysis with the A3G [E259Q] mutant did not yield any mutated sequences. The number of G-to-A/C-to-T mutations analyzed are as follows: HIV [p8.9]+A3G, $n=29$; HIV [p8.9]+A3G [W94A/W127A], $n=88$; *rpoB*+A3G, $n=30$; *rpoB*+A3G [W94A/W127A], $n=43$.

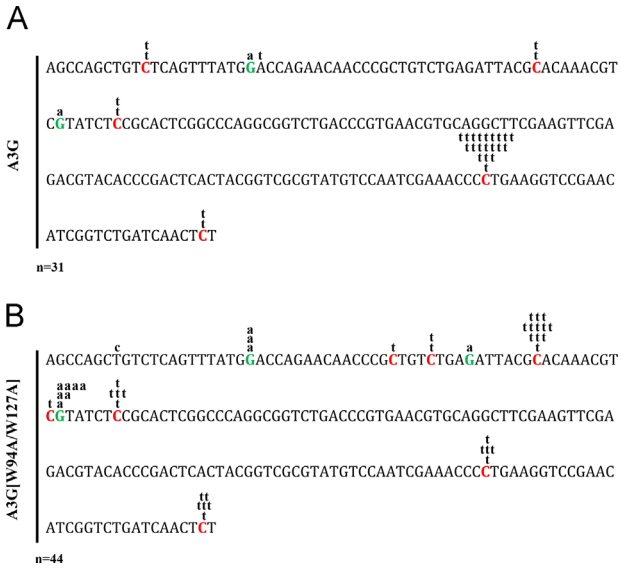

Fig. 3. Distribution of mutations in the *rpoB* gene of Rif^R *E. coli* expressing A3G or A3G [W94A/W127A]. Rif^R colonies generated by transforming *E.coli* with (**A**) GST-A3G or (B) GST-A3G [W94A/W127A] expression plasmids were randomly selected and their *rpoB* gene was amplified by PCR. Amplicons were then cloned and sent for sequencing. Mutated cytosines on the coding strand DNA are indicated in red and in green are mutated guanines; n indicates the total number of mutations in each library. Additional sequence information is presented in Table 1.

Overall, our results suggest that tryptophan to alanine substitutions at positions 94 and 127 of the NTD may affect the overall DNA substrate binding efficiency of the full length A3G protein. In fact, several published reports have speculated that W94 and W127 may interact with ssDNA substrates; residue W94 has been recently proposed to contact the DNA substrate in a full-length model of A3G (Lu et al., 2015), and moreover, the residue homologous to W94 in A3A (W98) has been shown to be directly involved in DNA binding (Logue et al., 2014). Furthermore, Chen et al. (2008) previously identified W285, which is homologous to W94 in the CTD of A3G, as an important contributor to DNA-binding. Substrate interactions with residues within the NTD could contribute to its positioning and stabilization for efficient deamination by the active site of the CTD. Finally, the W127A substitution has been shown to alter the scanning mechanism of the protein on ssDNA causing a decreased mutagenic potential, presumably because of the loss of protein homodimerization (Ara et al., 2014). Our experimental data therefore supports these studies by implicating both W94 and W127 in not only RNA binding, but also in physical interactions with the ssDNA substrate.

To date, the DNA dinucleotide preference of A3G has been attributed mainly to amino acids comprising loop 7 of the CTD of the protein. More specifically, Rathore et al. identified that residue D317 is responsible for α-helix capping resulting in restrained mobility of loop 7 and the generation of a binding pocket more favorable for the inclusion of cytosine than any other base (Rathore et al., 2013). In addition, according to the "brim model" for DNA binding, the initial engagement of the substrate has been proposed to occur via the NTD of A3G followed by a prolonged binding by the CTD that then carries out the deamination (Shindo et al., 2012). Because W127 is also located in loop 7 of the NTD of A3G, it is possible that mutations at positions 94 and 127 could destabilize the initial DNA substrate binding resulting in a less stringent substrate selection by the catalytic CTD. The crystal structure of full-length A3G bound to its ssDNA substrate would certainly help better understand this process.

Another factor that may also contribute to the loss of antiretroviral activity of the [W94A/W127A] mutant is the lack of deamination-independent restriction. We previously reported that both the W94A and W127A point mutants did not exhibit the typical features of deamination-independent restriction such as reduced late-reverse transcript accumulation and proviral integration (Bélanger et al., 2013). Although the same loss-of-function is expected of the double mutant, an antiretroviral feature that was not investigated is binding to the viral IN and RT. Interactions of A3G with these two viral proteins have previously been linked to reduced retroviral infection (Luo et al., 2007; Wang et al., 2012).

In order to address this question, HIV [p8.9] pseudoviruses were produced in the presence or absence of Flag-tagged APOBEC proteins followed by co-immunoprecipitation (co-IP) using anti-Flag-conjugated agarose beads. Viral proteins were detected in immunoprecipitates by Western blotting. Our results show an interaction between all the A3G mutants, including the double mutant, with both the viral RT and IN suggesting that the binding to the viral enzymes does not require RNA (Fig. 4A). Although [W94A/W127A] was not expressed as well as the point mutants or the wild type protein in presence of virus, the binding ratios to either RT or IN were comparable for all A3G proteins (Fig. 4B). We therefore find no evidence that the binding to IN or RT is sufficient to impede the efficiency of viral infection. However, these results may also indicate that interactions with IN and RT need to occur in conjunction to RNA or ssDNA binding by the NTD in order for A3G to exhibit deamination-independent restriction of retroviral infection.

Materials and methods

Antibodies and cells

Human embryonic kidney epithelium (HEK) 293T cells were cultured in HyClone DMEM/High Glucose medium (Thermo Fischer

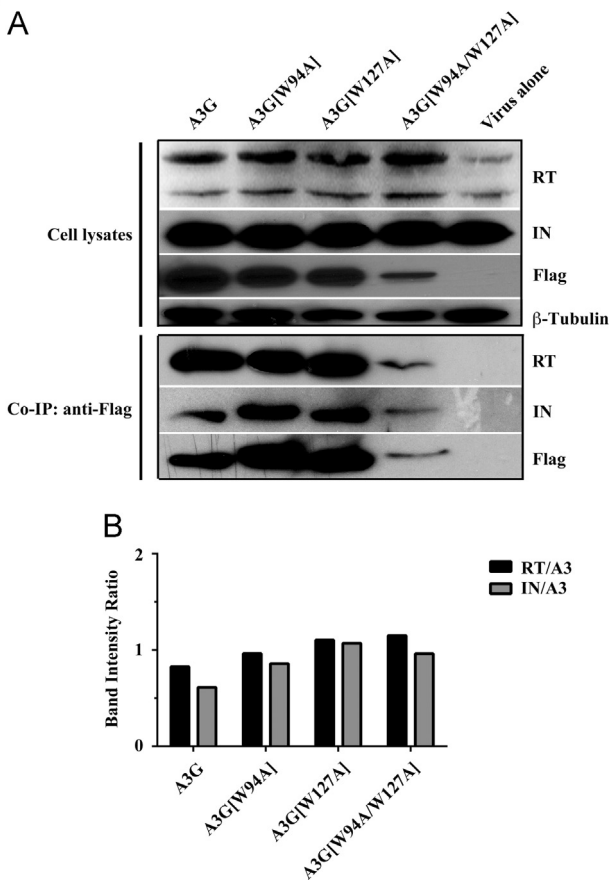

Fig. 4. Interaction of A3G and mutants with HIV-1 RT and IN. (A) HIV [p8.9] particles were produced in the presence of Flag-A3G or mutants of A3G by co-transfection in 293T cells. Cells were harvested 48 h after transfection and lysed for 30 min. Lysates were subjected to Co-IP analysis using anti-Flag-conjugated agarose beads. Following high-pH elution of the proteins from the agarose beads, precipitates were analyzed by Western blot and probed with anti-Flag, anti-IN and anti-RT antibodies. The amount of input cell lysate was normalized using β-tubulin expression. One representative Co-IP experiment of two is depicted. (B) Quantification of Western blot band intensities. Data is presented as the intensity ratio of the viral proteins (RT or IN) to the specific A3 proteins in each experimental condition. Ratios were calculated from the average band intensities from two independent Co-IP experiments.

Scientific) supplemented with 10% fetal bovine serum (FBS), 100U/ml penicillin and 100 μg/ml streptomycin (Multicell). The following antibodies were used for this study: HRP-conjugated anti-Flag (A8592, Sigma), anti-eGFP (no.632381, Clontech), anti-p24 (ab9069, Abcam) and HRP-conjugated anti-β-tubulin (ab21058,Abcam). The anti-Katα was provided by Dr. Stinzi from the University of Ottawa. The anti-HIV-1 integrase polyclonal and anti-HIV-1 reverse transcriptase polyclonal antibodies were obtained from the NIH AIDS Research Reference and Reagent Program (#757 and #6195 respectively) (Grandgenett and Goodarzi, 1994; Szilvay et al., 1992).

Plasmids

Flag-tagged and eGFP-tagged A3G and A2 expression plasmids were constructed previously (Langlois et al., 2005). Mutants of A3G were generated from the corresponding plasmids by PCR-based site directed mutagenesis as previously described (Bélanger et al., 2013).

The single-cycle HIV[p8.9] reporter pseudovirus has been described in previous reports (Bélanger et al., 2013; Langlois et al., 2005). Particles are produced by co-transfecting a Vif-deficient HIV-1 Gag-Pol expression plasmid (p8.9), a packageable HIV-1 LTR backbone containing the eGFP reporter gene under the control of an internal SFFV promoter (pCSGW), and a VSV-G expression vector (pMDG). For the bacterial pGST-expression plasmids, the coding sequences of A3G and A3G [W94A/W127A] were amplified by PCR from pFlag-APOBEC plasmids using the following primers; Xho1-FWD: 5′-GAATTCCCTCGAGGCCACCATGAAGCCTCACTTCAGAAAC-3′ and Pst1-REV: 5′-CGTCGACTGCAGTCAGTTTTCCTGATTCTGGA-3′. The PCR products were then digested and inserted in the pGST-2 vector (Addgene) using the Xho1 and Pst1 restriction sites.

Transfections and viral infectivity assays

Transfections and infections were conducted as described elsewhere (Bélanger et al., 2013). The packaging of APOBEC proteins inside viral particles was assayed by producing HIV [p8.9] viruses in the presence of eGFP-tagged APOBECs for 96 h. Virus-containing supernatants were then purified by ultra-centrifugation and pellets were resuspended in RIPA lysis buffer for Western blot analysis.

Velocity sedimentation

Velocity sedimentation analyses were conducted following the methods described in a previous report (Bélanger et al., 2013). Briefly, 293T cells expressing Flag-A2, Flag-A3G or Flag-A3G [W94A/W127A] were lysed for 30 min on ice with NP40 lysis buffer supplemented with a protease inhibitor cocktail (Roche). Half of each sample was then treated for 15 min at room temperature with 1 μg/mL of RNase A, and both treated and untreated samples were then loaded onto a 5–40% sucrose step gradient and resolved by ultra-centrifugation.

Fluorescence microscopy

Detailed procedures for this part can be found in (Bélanger et al., 2013). 293T cells were seeded in 35 mm glass bottom dishes (MatTech) and transfected with plasmids expressing eGFP-A3G or eGFP-A3G [W94A/W127A]. Images of live cells were captured using a Zeiss Axio Observer.Z1 inverted fluorescent microscope and a Plan-Apochromat 63x/1.4 oil immersion objective. Acquisition and deconvolution were performed using the AxioVision software (Zeiss).

Rif^R bacterial mutator assay

Bacterial mutator assays were performed as previously described (Bélanger et al., 2013). In brief, the *E. coli* uracil excision-defective strain BW310 was transformed with an empty pGST or an APOBEC-expressing pGST plasmid and plated overnight on ampicillin-containing plates. Single transformants were picked and used to inoculate 6 independent liquid media cultures supplemented with 1 mM IPTG and 100 μg/mL ampicillin. To obtain rifampicin resistant (Rif^R) mutants, 300 μL of each culture was spread onto low salt LB media containing 100 μg/mL ampicillin and 50 ug/mL rifampicin and incubated at 37 °C overnight.

For sequencing analysis, Rif^R colonies produced in presence of A3G or A3G [W94A/W127A] were diluted in 200 μl of water and 2 μl of the dilution was used in a PCR reaction mix with primers against a 198 bp region of the RNA polymerase B (*rpoB*) gene. PCR amplification was carried out by the PrimeStar HS high fidelity polymerase (Takara Bio Inc.). The sequence of the primers used for the amplifications are as follows: *rpoB*-FWD: 5′-TTGGCGAAATGGCG-GAAAACC-3′; *rpoB*-REV: 5′-CACCGACGGATACCACCTGCTG-3′. Cycling conditions were: 94 °C for 2 min, 94 °C for 30 sec, 65 °C for 1 min and 72 °C for 6 min. Steps 2 to 4 were repeated 8 times with a decrease of 1 °C in the annealing temperature (step 3) at every

successive cycle. That was followed by 21 cycles at 94 °C for 30 sec, 56 °C for 1 min and 72 °C for 5 min. PCR products were purified and sent for Sanger sequencing.

Immunoprecipitation

Methods for immunoprecipitation have been described in (Bélanger et al., 2013). Briefly, lysates of 293T cells transfected or co-transfected with Flag-APOBEC and HIV [p8.9] expression vectors were incubated for 3 h at 4 °C with anti-Flag conjugated agarose beads pre-treated with salmon sperm DNA (500 μg/ml). Bound complexes were then eluted from the beads with a high-pH buffer prior to RNA isolation or Western blot analysis.

RNA binding assay

Methods for RNA amplification and quantification were performed as described in previous reports (Bach et al., 2008; Bélanger et al., 2013). Briefly, RNA was purified from normalized quantities of Flag-tagged APOBEC immunoprecipitates using Trizol (Sigma). After DNAse treatment of the samples, RNA was reverse-transcribed using random hexamers and the ImProm-IITM reverse transcriptase according to the manufacturer's recommendations (Promega). The resulting cDNA was used for qPCR using GoTaq-Green Master Mix (Promega) and specific primers for 7SL, Alu, hY1, hY3 were used as previously described (Bach et al., 2008; Bélanger et al., 2013).

3D-PCR

This procedure is detailed in (Suspene et al. (2005)). Infected 293T cells were collected 24 h after infection for gDNA extraction and 3D-PCR was performed in a two-step protocol using the PrimeStar HS high fidelity polymerase (Takara Bio Inc.). A first-round PCR was performed to amplify a 717 bp eGFP amplicon using primers eGFP-FWD: 5′-GTGAGCAAGGGCGAGGAGCTGTTC-3′ and eGFP-REV:5′CTTGTACAGCTCGTCCATGCCGAGA-3′. A second-round 7-point gradient PCR targeting a 279 bp nested fragment within the eGFP sequence was then performed using primers R279-FWD: 5′–ACAACAGCCACAACGTCTATATCAT-3′ and 279-REV: 5′–CGTCCATGCCGAGAGTGAT-3′. The band of the gradient amplifying at the lowest temperature was then purified and cloned in the pBlueScript vector (Agilent Technologies). Independent clones were sequenced using M13 reverse primers and mutations computed on the plus-strand DNA.

HRM analysis

This method was detailed in a previous report by our group (Bélanger et al., 2014). The protocol was performed on 20 ng of gDNA isolated from virus-infected cells. A 717 bp eGFP amplicon was produced using the MeltDoctor Master Mix (Life Technologies) and the following primers: eGFP-FWD and eGFP-REV. qPCR and HRM were carried out on a ViiA™ 7 real-time PCR instrument (Applied Biosystems), and data was analyzed using the ViiA™ 7 system software (Applied Biosystems).

Protein self-association analysis

Pull-downs for eGFP epitope tags were performed according to the manufacturer's specifications detailed in the uMACS™ Epitope Tag Protein Isolation kits (Miltenyi Biotec).

Statistical analysis and software

All statistical analyses were performed using Student's paired *t*-test using GraphPad Prism software as previously described (Bélanger et al., 2013). Western blot band intensity analysis was performed using ImageJ.

Conclusions

Here we have demonstrated that A3G residues W94 and W127 together account for all detectable RNA binding by the protein. The dual substitution of these tryptophans to alanines resulted in a complete loss of retroviral restriction and in a very low frequency of hypermutated retroviral sequences recovered from infected target cells. Integrated proviral DNA sequences that were deaminated by the W94A/W127A mutant displayed a shift in preferred target sites from 5′CC to 5′TC. Reduced frequencies of hypermutated proviral sequences are not a reflection of reduced mutator activity by the A3G double mutant. Mutation assays in bacteria revealed that A3G [W94A/W127A] was as efficient as the wild type A3G protein, however with a sequence specificity that had also changed, but this time from 5′CC to 5′KC. These results highlight the essential role played by these RNA-binding residues in the efficient restriction and hypermutation of retroviruses. Detailed structural studies have only focused on the crystal of the CTD of A3G. As a consequence, there is still a very limited understanding of how the NTD interacts with both the ssDNA substrate and with the CTD active site of the enzyme. This study is the first to highlight the involvement of the NTD of A3G in influencing both the enzyme's substrate specificity and mutator activity on retroviral DNA.

Acknowledgments

The authors thank Tyler Renner for helpful discussions, and Kristin Kemmerich for comments on the manuscript. We are grateful to the NIH AIDS Research and Reference Reagent Program for reagents. K.B. holds an Ontario Graduate Scholarship and a scholarship from le Fonds de Recherche en Santé du Québec. M.-A. L. holds a Canada Research Chair in Molecular Virology and Intrinsic Immunity. This research was supported by grant #89774 from the Canadian Institutes of Health Research, and an Early Researcher Award from the Ontario Ministry of Research and Innovation to M.-A.L.

References

Ara, A., Love, R.P., Chelico, L., 2014. Different mutagenic potential of HIV-1 restriction factors APOBEC3G and APOBEC3F is determined by distinct single-stranded DNA scanning mechanisms. PLoS Pathog. 10, e1004024.

Armitage, A.E., Deforche, K., Chang, C.H., Wee, E., Kramer, B., Welch, J.J., Gerstoft, J., Fugger, L., McMichael, A., Rambaut, A., Iversen, A.K., 2012. APOBEC3G-induced hypermutation of human immunodeficiency virus type-1 is typically a discrete "all or nothing" phenomenon. PLoS Genet. 8, e1002550.

Bach, D., Peddi, S., Mangeat, B., Lakkaraju, A., Strub, K., Trono, D., 2008. Characterization of APOBEC3G binding to 7SL RNA. Retrovirology 5, 54.

Beale, R.C., Petersen-Mahrt, S.K., Watt, I.N., Harris, R.S., Rada, C., Neuberger, M.S., 2004. Comparison of the differential context-dependence of DNA deamination by APOBEC enzymes: correlation with mutation spectra in vivo. J. Mol. Biol.337, 585–596.

Bélanger, K., Savoie, M., Aydin, H., Renner, T.M., Montazeri, Z., Langlois, M.A., 2014. Deamination intensity profiling of human APOBEC3 protein activity along the near full-length genomes of HIV-1 and MoMLV by HyperHRM analysis. Virology 448, 168–175.

Bélanger, K., Savoie, M., Rosales Gerpe, M.C., Couture, J.F., Langlois, M.A., 2013. Binding of RNA by APOBEC3G controls deamination-independent restriction of retroviruses. Nucleic Acids Res. 41, 7438–7452.

Bishop, K.N., Holmes, R.K., Malim, M.H., 2006. Antiviral potency of APOBEC proteins does not correlate with cytidine deamination. J. Virol. 80, 8450–8458.

Bishop, K.N., Verma, M., Kim, E.Y., Wolinsky, S.M., Malim, M.H., 2008. APOBEC3G inhibits elongation of HIV-1 reverse transcripts. PLoS Pathog. 4, e1000231.
Bohn, M.F., Shandilya, S.M., Albin, J.S., Kouno, T., Anderson, B.D., McDougle, R.M., Carpenter, M.A., Rathore, A., Evans, L., Davis, A.N., Zhang, J., Lu, Y., Somasundaran, M., Matsuo, H., Harris, R.S., Schiffer, C.A., 2013. Crystal structure of the DNA cytosine deaminase APOBEC3F: the catalytically active and HIV-1 Vif-binding domain. Structure 21, 1042–1050.
Bulliard, Y., Turelli, P., Rohrig, U.F., Zoete, V., Mangeat, B., Michielin, O., Trono, D., 2009. Functional analysis and structural modeling of human APOBEC3G reveal the role of evolutionarily conserved elements in the inhibition of human immunodeficiency virus type 1 infection and Alu transposition. J. Virol. 83, 12611–12621.
Byeon, I.J., Ahn, J., Mitra, M., Byeon, C.H., Hercik, K., Hritz, J., Charlton, L.M., Levin, J.G., Gronenborn, A.M., 2013. NMR structure of human restriction factor APOBEC3A reveals substrate binding and enzyme specificity. Nat. Commun. 4, 1890.
Carpenter, M.A., Rajagurubandara, E., Wijesinghe, P., Bhagwat, A.S., 2010. Determinants of sequence-specificity within human AID and APOBEC3G. DNA Repair9, 579–587.
Chen, K.M., Harjes, E., Gross, P.J., Fahmy, A., Lu, Y., Shindo, K., Harris, R.S., Matsuo, H., 2008. Structure of the DNA deaminase domain of the HIV-1 restriction factor APOBEC3G. Nature 452, 116–119.
Chiu, Y.L., Soros, V.B., Kreisberg, J.F., Stopak, K., Yonemoto, W., Greene, W.C., 2005. Cellular APOBEC3G restricts HIV-1 infection in resting CD4+T cells. Nature 435, 108–114.
Dang, Y., Wang, X., Esselman, W.J., Zheng, Y.H., 2006. Identification of APOBEC3DE as another antiretroviral factor from the human APOBEC family. J. Virol. 80, 10522–10533.
Desimmie, B.A., Delviks-Frankenberrry, K.A., Burdick, R.C., Qi, D., Izumi, T., Pathak, V.K., 2014. Multiple APOBEC3 restriction factors for HIV-1 and one Vif to rule them all. J. Mol. Biol.426, 1220–1245.
Doehle, B.P., Schafer, A., Cullen, B.R., 2005. Human APOBEC3B is a potent inhibitor of HIV-1 infectivity and is resistant to HIV-1 Vif. Virology 339, 281–288.
Gallois-Montbrun, S., Kramer, B., Swanson, C.M., Byers, H., Lynham, S., Ward, M., Malim, M.H., 2007. Antiviral protein APOBEC3G localizes to ribonucleoprotein complexes found in P bodies and stress granules. J. Virol. 81, 2165–2178.
Grandgenett, D.P., Goodarzi, G., 1994. Folding of the multidomain human immunodeficiency virus type-I integrase. Protein Sci.: Publ. Protein Soc. 3, 888–897.
Guo, F., Cen, S., Niu, M., Yang, Y., Gorelick, R.J., Kleiman, L., 2007. The interaction of APOBEC3G with human immunodeficiency virus type 1 nucleocapsid inhibits tRNA3Lys annealing to viral RNA. J. Virol. 81, 11322–11331.
Hache, G., Liddament, M.T., Harris, R.S., 2005. The retroviral hypermutation specificity of APOBEC3F and APOBEC3G is governed by the C-terminal DNA cytosine deaminase domain. J. Biol. Chem. 280, 10920–10924.
Harris, R.S., Bishop, K.N., Sheehy, A.M., Craig, H.M., Petersen-Mahrt, S.K., Watt, I.N., Neuberger, M.S., Malim, M.H., 2003. DNA deamination mediates innate immunity to retroviral infection. Cell 113, 803–809.
Harris, R.S., Dudley, J.P., 2015. APOBECs and virus restriction. Virology 479–480, 131–145.
Harris, R.S., Petersen-Mahrt, S.K., Neuberger, M.S., 2002. RNA editing enzyme APOBEC1 and some of its homologs can act as DNA mutators. Mol. Cell. 10, 1247–1253.
Huthoff, H., Autore, F., Gallois-Montbrun, S., Fraternali, F., Malim, M.H., 2009. RNA-dependent oligomerization of APOBEC3G is required for restriction of HIV-1. PLoS Pathog. 5, e1000330.
Huthoff, H., Malim, M.H., 2007. Identification of amino acid residues in APOBEC3G required for regulation by human immunodeficiency virus type 1 Vif and Virion encapsidation. J. Virol. 81, 3807–3815.
Iwatani, Y., Chan, D.S., Wang, F., Maynard, K.S., Sugiura, W., Gronenborn, A.M., Rouzina, I., Williams, M.C., Musier-Forsyth, K., Levin, J.G., 2007. Deaminase-independent inhibition of HIV-1 reverse transcription by APOBEC3G. Nucleic Acids Res. 35, 7096–7108.
Iwatani, Y., Takeuchi, H., Strebel, K., Levin, J.G., 2006. Biochemical activities of highly purified, catalytically active human APOBEC3G: correlation with antiviral effect. J. Virol. 80, 5992–6002.
Jarmuz, A., Chester, A., Bayliss, J., Gisbourne, J., Dunham, I., Scott, J., Navaratnam, N., 2002. An anthropoid-specific locus of orphan C to U RNA-editing enzymes on chromosome 22. Genomics 79, 285–296.
Khan, M.A., Goila-Gaur, R., Opi, S., Miyagi, E., Takeuchi, H., Kao, S., Strebel, K., 2007. Analysis of the contribution of cellular and viral RNA to the packaging of APOBEC3G into HIV-1 virions. Retrovirology 4, 48.
Kitamura, S., Ode, H., Nakashima, M., Imahashi, M., Naganawa, Y., Kurosawa, T., Yokomaku, Y., Yamane, T., Watanabe, N., Suzuki, A., Sugiura, W., Iwatani, Y., 2012. The APOBEC3C crystal structure and the interface for HIV-1 Vif binding. Nat. Struct. Mol. Biol. 19, 1005–1010.
Kohli, R.M., Abrams, S.R., Gajula, K.S., Maul, R.W., Gearhart, P.J., Stivers, J.T., 2009. A portable hot spot recognition loop transfers sequence preferences from APOBEC family members to activation-induced cytidine deaminase. J. Biol. Chem. 284, 22898–22904.
Kohli, R.M., Maul, R.W., Guminski, A.F., McClure, R.L., Gajula, K.S., Saribasak, H., McMahon, M.A., Siliciano, R.F., Gearhart, P.J., Stivers, J.T., 2010. Local sequence targeting in the AID/APOBEC family differentially impacts retroviral restriction and antibody diversification. J. Biol. Chem. 285, 40956–40964.
Kozak, S.L., Marin, M., Rose, K.M., Bystrom, C., Kabat, D., 2006. The anti-HIV-1 editing enzyme APOBEC3G binds HIV-1 RNA and messenger RNAs that shuttle between polysomes and stress granules. J. Biol. Chem. 281, 29105–29119.
Langlois, M., Beale, R., Conticello, S., Neuberger, M., 2005. Mutational comparison of the single-domained APOBEC3C and double-domained APOBEC3F/G anti-retroviral cytidine deaminases provides insight into their DNA target site specificities. Nucleic Acids Res. 33, 1913–1923.
LaRue, R.S., Andresdottir, V., Blanchard, Y., Conticello, S.G., Derse, D., Emerman, M., Greene, W.C., Jonsson, S.R., Landau, N.R., Lochelt, M., Malik, H.S., Malim, M.H., Munk, C., O'Brien, S.J., Pathak, V.K., Strebel, K., Wain-Hobson, S., Yu, X.F., Yuhki, N., Harris, R. S., 2009. Guidelines for naming nonprimate APOBEC3 genes and proteins. J. Virol. 83, 494–497.
Lavens, D., Peelman, F., Van der Heyden, J., Uyttendaele, I., Catteeuw, D., Verhee, A., Van Schoubroeck, B., Kurth, J., Hallenberger, S., Clayton, R., Tavernier, J., 2010. Definition of the interacting interfaces of Apobec3G and HIV-1 Vif using MAPPIT mutagenesis analysis. Nucleic Acids Res. 38, 1902–1912.
Lecossier, D., Bouchonnet, F., Clavel, F., Hance, A.J., 2003. Hypermutation of HIV-1 DNA in the absence of the Vif protein. Science 300, 1112.
Li, X.Y., Guo, F., Zhang, L., Kleiman, L., Cen, S., 2007. APOBEC3G inhibits DNA strand transfer during HIV-1 reverse transcription. J. Biol. Chem. 282, 32065–32074.
Liddament, M.T., Brown, W.L., Schumacher, A.J., Harris, R.S., 2004. APOBEC3F properties and hypermutation preferences indicate activity against HIV-1 in vivo. Curr. Biol.: CB 14, 1385–1391.
Logue, E.C., Bloch, N., Dhuey, E., Zhang, R., Cao, P., Herate, C., Chauveau, L., Hubbard, S.R., Landau, N.R., 2014. A DNA sequence recognition loop on APOBEC3A controls substrate specificity. PloS One 9, e97062.
Lu, X., Zhang, T., Xu, Z., Liu, S., Zhao, B., Lan, W., Wang, C., Ding, J., Cao, C., 2015. Crystal structure of DNA cytidine deaminase abobec3g catalytic deamination domain suggests a binding mode of full-length enzyme to single-stranded DNA. J. Biol. Chem. 290, 4010–4021.
Luo, K., Wang, T., Liu, B., Tian, C., Xiao, Z., Kappes, J., Yu, X.F., 2007. Cytidine deaminases APOBEC3G and APOBEC3F interact with human immunodeficiency virus type 1 integrase and inhibit proviral DNA formation. J. Virol. 81, 7238–7248.
Mangeat, B., Turelli, P., Liao, S., Trono, D., 2004. A single amino acid determinant governs the species-specific sensitivity of APOBEC3G to Vif action. J. Biol. Chem. 279, 14481–14483.
Mariani, R., Chen, D., Schrofelbauer, B., Navarro, F., Konig, R., Bollman, B., Munk, C., Nymark-McMahon, H., Landau, N.R., 2003. Species-specific exclusion of APOBEC3G from HIV-1 virions by Vif. Cell 114, 21–31.
Mbisa, J.L., Bu, W., Pathak, V.K., 2010. APOBEC3F and APOBEC3G inhibit HIV-1 DNA integration by different mechanisms. J. Virol. 84, 5250–5259.
Navarro, F., Bollman, B., Chen, H., Konig, R., Yu, Q., Chiles, K., Landau, N.R., 2005. Complementary function of the two catalytic domains of APOBEC3G. Virology 333, 374–386.
Neuberger, M.S., Harris, R.S., Di Noia, J., Petersen-Mahrt, S.K., 2003. Immunity through DNA deamination. Trends Biochem. Sci. 28, 305–312.
Newman, E.N., Holmes, R.K., Craig, H.M., Klein, K.C., Lingappa, J.R., Malim, M.H., Sheehy, A.M., 2005. Antiviral function of APOBEC3G can be dissociated from cytidine deaminase activity. Curr. Biol.: CB 15, 166–170.
OhAinle, M., Kerns, J.A., Malik, H.S., Emerman, M., 2006. Adaptive evolution and antiviral activity of the conserved mammalian cytidine deaminase APOBEC3H. J. Virol. 80, 3853–3862.
Rathore, A., Carpenter, M.A., Demir, O., Ikeda, T., Li, M., Shaban, N.M., Law, E.K., Anokhin, D., Brown, W.L., Amaro, R.E., Harris, R.S., 2013. The local dinucleotide preference of APOBEC3G can be altered from 5′-CC to 5′-TC by a single amino acid substitution. J. Mol. Biol. 425, 4442–4454.
Schrofelbauer, B., Chen, D., Landau, N.R., 2004. A single amino acid of APOBEC3G controls its species-specific interaction with virion infectivity factor (Vif). Proc. Natl. Acad. Sci. USA 101, 3927–3932.
Shindo, K., Li, M., Gross, P.J., Brown, W.L., Harjes, E., Lu, Y., Matsuo, H., Harris, R.S., 2012. A comparison of two single-stranded DNA binding models by mutational analysis of APOBEC3G. Biology 1, 260–276.
Siu, K.K., Sultana, A., Azimi, F.C., Lee, J.E., 2013. Structural determinants of HIV-1 Vif susceptibility and DNA binding in APOBEC3F. Nat. Commun. 4, 2593.
Suspene, R., Henry, M., Guillot, S., Wain-Hobson, S., Vartanian, J.P., 2005. Recovery of APOBEC3-edited human immunodeficiency virus G- > A hypermutants by differential DNA denaturation PCR. J. Gen. Virol. 86, 125–129.
Suspene, R., Sommer, P., Henry, M., Ferris, S., Guetard, D., Pochet, S., Chester, A., Navaratnam, N., Wain-Hobson, S., Vartanian, J.P., 2004. APOBEC3G is a single-stranded DNA cytidine deaminase and functions independently of HIV reverse transcriptase. Nucleic Acids Res. 32, 2421–2429.
Szilvay, A.M., Nornes, S., Haugan, I.R., Olsen, L., Prasad, V.R., Endresen, C., Goff, S.P., Helland, D.E., 1992. Epitope mapping of HIV-1 reverse transcriptase with monoclonal antibodies that inhibit polymerase and RNase H activities. J. Acquir. Immune Defic. Syndr. 5, 647–657.
Wang, M., Rada, C., Neuberger, M.S., 2010. Altering the spectrum of immunoglobulin V gene somatic hypermutation by modifying the active site of AID. J. Exp. Med. 207, 141–153.
Wang, X., Ao, Z., Chen, L., Kobinger, G., Peng, J., Yao, X., 2012. The cellular antiviral protein APOBEC3G interacts with HIV-1 reverse transcriptase and inhibits its function during viral replication. J. Virol. 86, 3777–3786.
Wichroski, M.J., Robb, G.B., Rana, T.M., 2006. Human retroviral host restriction factors APOBEC3G and APOBEC3F localize to mRNA processing bodies. PLoS Pathog. 2, e41.
Yu, Q., Konig, R., Pillai, S., Chiles, K., Kearney, M., Palmer, S., Richman, D., Coffin, J.M., Landau, N.R., 2004. Single-strand specificity of APOBEC3G accounts for minus-strand deamination of the HIV genome. Nat. Struct. Mol. Biol. 11, 435–442.